Journal of Computational Physics 367 (2018) 87–101

Contents lists available at ScienceDirect

Journal of Computational Physics

www.elsevier.com/locate/jcp

Nonlocal PDF methods for Langevin equations with colored noise

Tyler Maltba [a,1], Pierre A. Gremaud [b,1,*], Daniel M. Tartakovsky [c,2]

[a] Department of Statistics, UC Berkeley, Berkeley, CA 94720, USA
[b] Department of Mathematics, North Carolina State University, Raleigh, NC 27695, USA
[c] Department of Energy Resources Engineering, Stanford University, Stanford, CA 94305, USA

ARTICLE INFO

Article history:
Received 29 August 2017
Received in revised form 27 March 2018
Accepted 11 April 2018
Available online 13 April 2018

Keywords:
PDF method
Nonlocal
Langevin equation
Colored noise
Stochastic
Random
Uncertainty quantification

ABSTRACT

Langevin equations describe systems driven by internally generated or externally imposed random excitations. If these excitations correspond to Gaussian white noise, it is relatively straightforward to derive a closed form equation for the joint probability density function (PDF) of state variables. Many natural phenomena present however correlated (colored) excitations. For such problems, a full probabilistic characterization through the resolution of a PDF equation can be obtained through two levels of approximations: first, mixed ensemble moments have to be approximated to lead to a closed system of equations and, second, the resulting nonlocal equations should be at least partially localized to ensure computational efficiency. We propose a new semi-local formulation based on a modified large-eddy diffusivity (LED) approach; the formulation retains most of the accuracy of a fully nonlocal approach while presenting the same order of algorithmic complexity as the standard LED approach. The accuracy of the approach is successfully tested against Monte Carlo simulations.

1. Introduction

Randomness enters mathematical models either through stochastic forcing terms accounting for "sub-grid" fluctuations or probabilistic representations of uncertain coefficients. These sources of randomness are inherent to most–if not all–models of complex phenomena. Analyzing and quantifying the effects of randomness on system behavior is thus central not only to the analysis of Langevin equations but also to mathematical modeling in general.

Monte Carlo simulations (MCS) are often used to solve stochastic problems through the computation of a few statistical moments of a system state such as ensemble mean and variance. They are robust, easy to implement and readily parallelizable, yet computationally demanding. The search for more efficient alternatives has led to the development of quasi-MCS, moment differential equations (MDE), polynomial chaos expansions (PCE), and the method of distributions. These and other methods have their respective strengths and limitations, e.g., MDE typically require closure approximations that formally limit their applicability to small coefficients of variation of the random inputs; and PCE approximate the spatiotemporally varying inputs with a finite number of random variables, which renders them unsuitable for problems whose coefficients

* Corresponding author.
E-mail addresses: tyler_maltba@berkeley.edu (T. Maltba), gremaud@ncsu.edu (P.A. Gremaud), tartakovsky@stanford.edu (D.M. Tartakovsky).
[1] Supported by the National Science Foundation award DMS-1522765.
[2] Supported by the National Science Foundation award DMS-1522799.

and sources are uncorrelated random functions (fields or processes) or have short-range correlations such as Langevin equations driven by either white or colored noise.

A model with random coefficients and/or random driving forces admits multiple solutions, the likelihood of which can be characterized by the probability density function (PDF) or the cumulative distribution function (CDF) of the system state. The method of distributions, which comprises PDF and CDF methods, aims to derive a deterministic (partial differential) equation for the PDF (or CDF) of a system state; when the dynamics of a system state is governed by a Langevin equation, the corresponding PDF equation is referred to as a Fokker–Planck equation. The PDF method has its origins in statistical theory of turbulence [1] and has since been adapted to quantify parametric uncertainty in hyperbolic [2, and the references therein] and parabolic [3] partial differential equations, as well as to derive Fokker–Planck equations for Langevin systems driven by colored noise [4]. The method of distribution is often exact for white-noise inputs[3] but, in general, requires closure approximations when inputs are random fields exhibiting spatiotemporal correlations. Thus, the method of distributions is complementary to PCE in the sense that the performance of its closures generally improves as input correlation lengths decrease [2].

The need for closures stems from the stochastic averaging of differential equations with multiplicative noise; they typically involve two approximations. The first one consists of approximating the mixed ensemble moments of the random parameters and system state. The second involves localization of the resulting PDF/CDF equation to replace an integro-differential equation with a partial differential equation. While the former approximation is necessary to render a PDF/CDF equation computable, the latter is used largely for computational expediency (see, e.g., the use of a large-eddy diffusivity closure [7] to derive Fokker–Planck-type equations for both Langevin equations with colored noise [4] and advection–reaction equations with uncertain parameters [8]).

Nonlocality is a salient feature of averaged systems, accounting for, e.g., non-Fickian or "anomalous" behavior of diffusion in crowded heterogeneous environments [9]. While the effects of localization on solutions of stochastically averaged differential equations have been studied in the past (e.g., [10]), we are not aware of similar analyses of the localization errors for PDF/CDF equations. A major goal of the present study is to fill this void. We apply the proposed approach to stochastic, Langevin-type systems driven by correlated (colored) noise in Section 2. The challenges inherent to closing the resulting systems of equations are discussed in Section 3 and in the Appendix. Section 4 describes proposed numerical methods to solve these systems along with their algorithmic complexity. In Section 5, we study the localization errors on two computational examples: Brownian particles driven by colored noise [11] and the stochastically forced Van der Pol oscillator. Main conclusions derived from our study are summarized in Section 6.

2. PDF method

Consider the random ordinary differential equation

$$\frac{d\mathbf{x}(t,\omega)}{dt} = \mathbf{v}(\mathbf{x}(t,\omega), t, \omega), \tag{1}$$

$$\mathbf{x}(0,\omega) = \mathbf{x}^0(\omega), \tag{2}$$

where the problem is to be solved on a time interval $(0, T_f)$ and (1), (2) are to hold for almost every $\omega \in \Omega$ with $(\Omega, \mathscr{F}, \mathbb{P})$ being an appropriate probability space. The solution $\mathbf{x}: (0, T_f) \times \Omega \to \mathbb{R}^N$ is an $\mathbb{R}^N$-valued stochastic process

$$\mathbf{x}(t,\omega) = [x_1(t,\omega), ..., x_N(t,\omega)]^T,$$

and $\mathbf{v}: \mathbb{R}^N \times (0, T_f) \times \Omega$ is a given continuous function. The initial condition $\mathbf{x}^0$ is an N-dimensional random vector. Denoting by $\langle\cdot\rangle \equiv \mathbb{E}[\cdot]$ the ensemble mean, we consider the Reynolds decomposition of $\mathbf{v} = [v_1, ..., v_N]^T$ into its deterministic part $\langle\mathbf{v}\rangle$ and a stochastic fluctuation $\mathbf{v}'$

$$\mathbf{v} = \langle\mathbf{v}\rangle + \mathbf{v}',$$

where $\mathbf{v}'$ has mean zero for any fixed $\mathbf{x}$ and t. The stochastic fluctuation term is characterized by its correlation time τ and finite characteristic amplitude. We assume that $\mathbf{v}$ satisfies additional conditions guaranteeing the existence of a unique path-wise solution to (1), (2) (see for instance [12,13]). In this paper, we concentrate on dynamical systems for which the effect of a nonzero correlation time of the stochastic fluctuation cannot be ignored.

Let $\mathbf{X} = [X_1, ..., X_N]^T \in \mathbb{R}^N$ be a variable in the system's phase space. At any given time t, the state of the system is characterized by the joint probability $\mathbb{P}[\mathbf{x}(t,\omega) \leq \mathbf{X}]$ or, equivalently, by its joint probability density function (PDF) $p(\mathbf{X}, t)$. We aim to derive a computable closed-form PDF equation for the initial value problem (IVP) (1), (2).

Let Π be the auxiliary function ("raw" PDF, [2])

$$\Pi(\mathbf{X}, t; \omega) = \delta(\mathbf{x}(t, \omega) - \mathbf{X}) = \prod_{i=1}^{N} \delta(x_i(t, \omega) - X_i), \tag{3}$$

with its corresponding Reynolds decomposition $\Pi = \langle \Pi \rangle + \Pi'$. By elementary properties of the Dirac delta function, the ensemble mean of $\Pi(\mathbf{X}, t)$ over all realizations of $\mathbf{x}$ at time t is simply the PDF $p(\mathbf{X}, t)$

$$\langle \Pi(\mathbf{X}, t) \rangle \equiv \int_{\mathbb{R}^N} \delta(\mathbf{Y} - \mathbf{X})\, p(\mathbf{Y}, t) d\mathbf{Y} = p(\mathbf{X}, t);$$

hence, $\Pi = p + \Pi'$.

Differentiating Π with respect to time yields the following conservation law

$$\frac{\partial \Pi}{\partial t} + \nabla_{\mathbf{X}} \cdot (\mathbf{v}\Pi) = 0, \tag{4}$$

where we have used (1), (3) and the sifting property of the Dirac delta function. Taking the ensemble mean of (4) and using the fact that $\langle \mathbf{v}' \rangle = 0$ leads to an initial boundary value problem for the PDF p

$$\frac{\partial p}{\partial t} + \nabla_{\mathbf{X}} \cdot (\langle \mathbf{v} \rangle p) + \nabla_{\mathbf{X}} \cdot \langle \mathbf{v}' \Pi' \rangle = 0, \tag{5}$$

$$p(\cdot, 0) = p^0, \tag{6}$$

with vanishing free-space boundary conditions. The initial condition (6) results from our assumed knowledge of the distribution of $\mathbf{x}^0$ in (2). The average flux term $\langle \mathbf{v}' \Pi' \rangle$ in (5) is unknown and can only be evaluated if the solution of the IVP in (1), (2) is known; in other words, the above problem is unclosed.

3. Closures

Our approach to closure follows that of [14]. For the sake of completeness, we present the details of the derivation of three possible closures, namely, nonlocal, semi-local and local, at the end of the paper, see Appendix A. In all three formulations, the terminal problem

$$\frac{d\boldsymbol{\chi}}{ds} = \langle \mathbf{v}(\boldsymbol{\chi}, s) \rangle, \tag{7}$$

$$\boldsymbol{\chi}(t) = \mathbf{X}, \tag{8}$$

and its associated flow $\boldsymbol{\chi}(s) = \boldsymbol{\Phi}(s; \mathbf{X}, t)$ play an essential role. Whenever possible, we drop ω from the notation for convenience.

The *local closure* is obtained by a direct application of the classical large-eddy diffusivity (LED) approach. Under that approach, the cross covariance term can be split into a drift velocity term and a diffusive term

$$\langle \mathbf{v}' \Pi' \rangle(\mathbf{X}, t) \approx \mathscr{V}(\mathbf{X}, t) p(\mathbf{X}, t) - \mathscr{D}(\mathbf{X}, t) \nabla_{\mathbf{X}} p(\mathbf{X}, t),$$

where the LED drift velocity $\mathscr{V}$ and the LED diffusion tensor $\mathscr{D}$ are given in (A.12) and (A.13) respectively. The range of validity of this closure is expected to be limited to short correlation time scales.

The *nonlocal closure* does not rely on short correlations; it is derived in the Appendix and takes the form

$$\langle \mathbf{v}' \Pi' \rangle(\mathbf{X}, t) \approx -\int_0^t \mathscr{J}(s; \mathbf{X}, t) \nabla_{\boldsymbol{\Phi}} \cdot \left(\left\langle \mathbf{v}'(\mathbf{X}, t) \mathbf{v}'^{T}(\boldsymbol{\Phi}(s; \mathbf{X}, t), s) \right\rangle p(\boldsymbol{\Phi}(s; \mathbf{X}, t), s) \right) ds, \tag{9}$$

where

$$\mathscr{J}(s; \mathbf{X}, t) = \exp\left(-\int_s^t \nabla_{\boldsymbol{\chi}} \cdot \langle \mathbf{v}(\boldsymbol{\chi}(\tau), \tau) \rangle \, d\tau \right). \tag{10}$$

When considering more accurate closures than a simple local approximation as above, the computational complexity of the PDF method for a given dimension N depends largely upon the work associated with solving the terminal problem (7), (8) and that of evaluating the Jacobian (10). Problems for which the divergence of the flow $\nabla_{\boldsymbol{\chi}} \cdot \langle \mathbf{v} \rangle$, which appears prominently in (10), is linear in $\boldsymbol{\chi}$ are dramatically simpler than the generic case. The Brownian particle application from Section 5 falls in this simplified category while the Van der Pol oscillator, also treated in Section 5, does not. In fact, several

classical test problems from the literature, such as the nonlinear pendulum and the Duffing oscillator fall in the special category of presenting a nonlinear flow but a linear flow divergence, see for instance [15]. These latter test problems are likely to give an overly optimistic assessment of the methods under consideration.

We explore here instead a modified LED closure which combines the simplicity and speed of the local one with (most of) the accuracy of the nonlocal one. Following [14], we construct a *semi-local* LED closure based on the mean-field advection problem

$$\frac{\partial p}{\partial s} + \nabla_{\mathbf{X}} \cdot (\langle \mathbf{v} \rangle\, p) = 0, \quad s < t, \tag{11}$$

$$p(\mathbf{\Phi}(s; \mathbf{X}, t), s) = \mathscr{J}^{-1}(s; \mathbf{X}, t) p(\mathbf{X}, t). \tag{12}$$

Equation (12) gives a local approximation for p; substituting it into the above nonlocal form of the cross covariance term, we obtain the semi-local closure

$$\langle \mathbf{v}' \Pi' \rangle (\mathbf{X}, t) \approx -\int_0^t \mathscr{J}(s; \mathbf{X}, t) \nabla_{\mathbf{\Phi}} \cdot \left(\left\langle \mathbf{v}'(\mathbf{X}, t) \mathbf{v}'^{T}(\mathbf{\Phi}(s; \mathbf{X}, t), s) \right\rangle \mathscr{J}^{-1}(s; \mathbf{X}, t) p(\mathbf{X}, t)] \right) ds. \tag{13}$$

The PDF p in (13) has been localized from $(\mathbf{\Phi}(s; \mathbf{X}, t), s)$ to $(\mathbf{X}, t)$ but the operator $\nabla_{\mathbf{\Phi}} \cdot$ has not.

4. Numerics

For any of the above closures, we solve (5) through Strang splitting by successively considering the two equations

$$\frac{\partial p}{\partial t} + \langle \mathbf{v} \rangle \cdot \nabla p = 0, \tag{14}$$

$$\frac{\partial p}{\partial t} + p \nabla \cdot \langle \mathbf{v} \rangle + \nabla \cdot \langle \mathbf{v}' \Pi' \rangle = 0. \tag{15}$$

The linear hyperbolic equation (14) is solved through the adaptive version of the Clawpack package [16] using a Lax–Wendroff discretization and a van Leer limiter. Equation (15) is solved through a Crank–Nicolson discretization (forward Euler for the nonlocal closure) and second-order central differencing in space.

The computational domain is taken as $(-L, L)^2$ where $L > 0$ is the smallest number large enough to ensure that the domain truncation, i.e., imposing extrapolated boundary conditions rather than $\lim_{|\mathbf{X}| \to \infty} p(\mathbf{X}) = 0$, only generates negligible errors (by which we mean that if the size of each dimension of the domain is increased 10 fold, the error improves only by 0.01 percent).

To compare the complexity attached to each of the three proposed closures, we consider a simplified numerical scheme built on a fixed uniform spatial mesh with n^2 spatial nodes in conjunction with forward Euler time-stepping. Let nt be the total number of time steps. Assuming a parabolic stability condition, nt is of order n^2, i.e., $nt = \mathcal{O}(n^2)$. For both the local and semi-local formulations, the computation of the required finite difference approximations requires $\mathcal{O}(n^2)$ operations at each time step. Repeating these operations nt time steps results in a complexity of $\mathcal{O}(n^4)$.

For the nonlocal formulation, unlike the local and semi-local ones, the evaluation of the divergence of the cross covariance term (9) usually involves a numerical approximation of the integral; this requires the history of the solution up to the current time step. To evaluate the integrand in (9), a second-order central finite difference function can be used. Characteristic tracing requires $\mathcal{O}(n)$ operations per node. Since there are a total of n^2 spatial nodes, evaluating the integrand of (9) requires $\mathcal{O}(n^3)$ operations. Considering the mth time step, the time integral in (9) is evaluated with $m+1$ quadrature nodes, i.e., evaluating the integral requires $(m+1) \cdot \mathcal{O}(n^3)$ operations. Summing over all time steps gives a total of

$$\mathcal{O}(n^3) \cdot \sum_1^{nt} (m+1) = \mathcal{O}(n^3) \cdot \left(\frac{nt\,(nt+3)}{2} \right) \tag{16}$$

operations for the nonlocal scheme. Hence, the nonlocal scheme has a complexity of $\mathcal{O}(n^7)$. Note that even if a fixed number of quadrature nodes were used in approximating the integral (at the price of a significant loss in accuracy), the complexity of the nonlocal scheme would still be $\mathcal{O}(n^5)$ versus $\mathcal{O}(n^4)$ for the local and semi-local formulations.

In the results presented below, the proposed semi-local approach is four orders of magnitude faster than as the standard Monte Carlo approach.

5. Applications

We consider two applications of the PDF method and its associated closures, namely, the motion of a free Brownian particle in water, and the Van der Pol oscillator with stochastic forcing, all driven by colored noise. Both applications have two state variables, i.e., $N = 2$.

5.1. Brownian particle

We consider a free silica microsphere of diameter of 1 μm in water at normal pressure and constant temperature $T = 293.15$ K. Under these conditions, the mean-field terminal problem (7), (8) has an analytic solution, eliminating additional numerical errors, and making it possible to concentrate our attention on the accuracy of the closures themselves.

For simplicity, we assume that the motion of the particle's center of mass, denoted by x, is one-dimensional. The motion is described by the stochastic Newton equation [11]

$$m\ddot{x} = -\gamma\dot{x} + \gamma\sqrt{\frac{2d}{\tau}}\xi_t \tag{17}$$

with some given initial conditions, deterministic or random. In (17), m is the mass of the considered particle, γ corresponds to friction as given by Stokes law, i.e., $\gamma = 6\pi\mu R$, R being the radius of the particle. The diffusion coefficient d is related to the friction coefficient γ by the fluctuation–dissipation relation:

$$d = \frac{k_B T}{\gamma}$$

where k_B is the Boltzmann constant. Finally, the colored noise ξ_t is taken to be an Ornstein–Uhlenbeck process defined by the stochastic differential equation (SDE):

$$d\xi_t = -\frac{2}{\tau}\xi_t\, dt + \sqrt{\frac{4}{\tau}}dW_t, \tag{18}$$

where τ is the noise correlation time and W_t is a standard Wiener process. The nonstationary solution to (18) is conditionally given by a scaled time-transformed Wiener process:

$$\xi_t = \xi_0 \exp\left(-\frac{2t}{\tau}\right) + \exp\left(-\frac{2t}{\tau}\right) W_{\exp\left(\frac{4t}{\tau}\right)-1},$$

or unconditionally given by

$$\xi_t = \exp\left(-\frac{2t}{\tau}\right) W_{\exp\left(\frac{4t}{\tau}\right)},$$

where $\langle\xi_t\rangle = 0$ for any fixed time t. Its associated covariance function is given by

$$C(t,s) = \exp\left(-\frac{2}{\tau}|t-s|\right) - \exp\left(-\frac{2}{\tau}(t+s)\right). \tag{19}$$

The characteristic value of the particle's relaxation time $\sigma = m/\gamma$ is given by $\sigma_0 = 0.11$ μs and the root mean square velocity is about $v_0 = 2\ \frac{\text{mm}}{\text{s}}$ [17]. Nondimensionalizing (17) with respect to σ_0, v_0, and $l_0 = \sigma_0 v_0$, and letting $x_1 = x$ and $x_2 = \dot{x}$, we arrive at a system of first-order Langevin equations:

$$\begin{bmatrix}\dot{x}_1\\ \dot{x}_2\end{bmatrix} = \begin{bmatrix}x_2\\ -x_2\end{bmatrix} + \hat{\xi}_t \begin{bmatrix}0\\ \sqrt{\frac{2d}{\tau v_0^2}}\end{bmatrix} \tag{20}$$

where $\hat{\xi}_t = \xi_{\sigma_0 t}$.

In the simulations below, we consider the following values of the correlation time $\tau = 10^{-8}$, 10^{-6}, and 10^{-4}. The initial condition (6) is taken as a zero-mean uncorrelated joint Gaussian:

$$p^0 \sim \mathcal{N}\left(\begin{bmatrix}0\\0\end{bmatrix}, \begin{bmatrix}\frac{2}{15}^2 & 0\\ 0 & \frac{2}{15}^2\end{bmatrix}\right).$$

5.1.1. Local closure

Applying the PDF method with the *local closure* to equation (20) results in the classical closed-form LED IBVP for the joint PDF p, given by equation (A.14). In this case, the LED drift velocity (A.12) and diffusion tensor (A.13) can be found exactly

$$\mathscr{V}(\mathbf{X},t) \equiv \begin{bmatrix}0\\0\end{bmatrix},$$

$$\mathscr{D}(\mathbf{X},t) \equiv \int_0^t \mathscr{J}(s;\mathbf{X},t)\left\langle \mathbf{v}'(\mathbf{X},t)\mathbf{v}'^{T}(\mathbf{\Phi}(s;\mathbf{X},t),s)\right\rangle ds = D_1(t)\begin{bmatrix}0 & 0\\ 0 & 1\end{bmatrix}$$

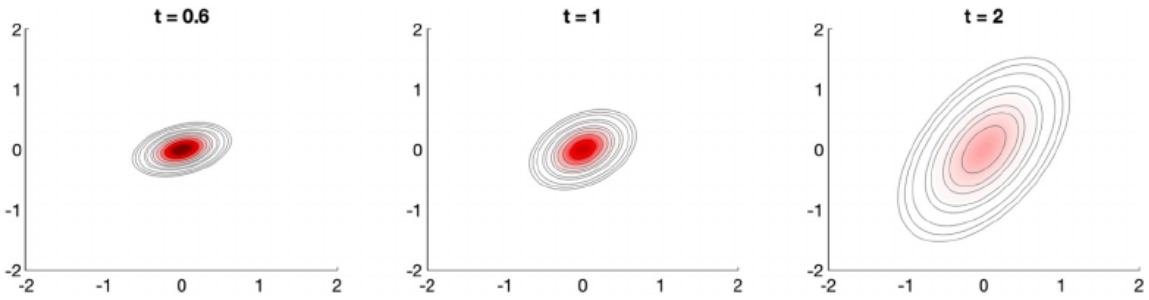

Fig. 1. Evolution of the joint PDF, computed through local closure, for the position (horizontal) and velocity (vertical) corresponding to (20) for a correlation time of $\tau = 10^{-6}$.

where

$$D_1(t) = \left(\frac{2d}{\tau v_0^2}\right)\int_0^t \mathscr{J}(s;\mathbf{X},t)C(\sigma_0 t,\sigma_0 s)\,ds = \left(\frac{2d}{\tau v_0^2}\right)\int_0^t \exp(t-s)C(\sigma_0 t,\sigma_0 s)\,ds$$

$$= \frac{2k_B T}{\gamma v_0^2}\Big(A + B\exp(\beta t) - (A+B)\exp(\alpha_1 t)\Big), \tag{21}$$

with $A = 1/(2\sigma_0 - \tau)$, $B = 1/(2\sigma_0 + \tau)$, $\alpha_1 = 1 - 2\sigma_0/\tau$, and $\beta = -4\sigma_0/\tau$. The classical closed-form LED IBVP for the joint PDF p, given by equation (A.14), then simplifies to

$$\partial_t p + x_2\,\partial_{x_1} p - x_2\,\partial_{x_2} p = p + D_1(t)\partial_{x_2 x_2} p$$

where $D_1(t)$ is given by (21). Fig. 1 displays the evolution of the joint PDF for the classical closed-form LED IBVP.

5.1.2. Semi-local closure

Applying the *semi-local closure* to equation (20) results in the closed-form IBVP for the PDF p given by (5), (6) where the cross covariance term is approximated by (13). Here, the expression from (13) can be found exactly

$$\langle \mathbf{v}'\Pi'\rangle \approx -\int_0^t \mathscr{J}(s;\mathbf{X},t)\nabla_{\mathbf{\Phi}}\cdot\Big(\Big\langle \mathbf{v}'(\mathbf{X},t)\mathbf{v}'^T(\mathbf{\Phi}(s;\mathbf{X},t),s)\Big\rangle \mathscr{J}^{-1}(s;\mathbf{X},t)p(\mathbf{X},t)]\Big)\,ds$$

$$= -\int_0^t \Big\langle \mathbf{v}'(\mathbf{X},t)\mathbf{v}'^T(\mathbf{\Phi}(s;\mathbf{X},t),s)\Big\rangle \nabla_{\mathbf{\Phi}}\, p(\mathbf{X},t)\,ds$$

$$= -\frac{2d}{\tau v_0^2}\int_0^t C(\sigma_0 t,\sigma_0 s)\begin{bmatrix}0\\ \partial_{\Phi_2} p(\mathbf{X},t)\end{bmatrix} ds. \tag{22}$$

As the terminal value problem (7), (8) is linear for the application under consideration, the characteristics Φ_1 and Φ_2 can also be computed exactly

$$\Phi_1(s;x_1,x_2,t) = -x_2\exp(t-s) + x_2 + x_1,$$
$$\Phi_2(s;x_1,x_2,t) = x_2\exp(t-s).$$

Under the substitution

$$\partial_{\Phi_2} = \exp(s-t)\partial_{x_2} \tag{23}$$

equation (22) becomes

$$\langle \mathbf{v}'\Pi'\rangle \approx -\begin{bmatrix}0\\ D_2(t)\end{bmatrix}\partial_{x_2} p$$

where

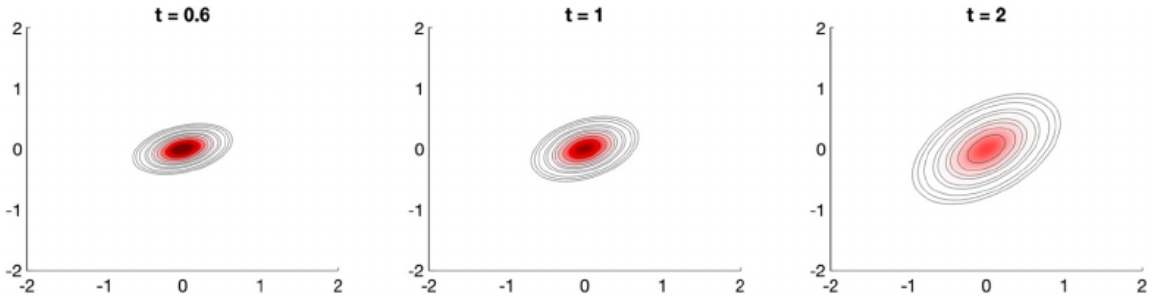

Fig. 2. Evolution of the joint PDF, computed through semi-local closure, for the position (horizontal) and velocity (vertical) corresponding to (20) for a correlation time of $\tau = 10^{-6}$.

$$D_2(t) = \frac{2d}{\tau v_0^2}\int_0^t \exp(s-t)C(\sigma_0 t, \sigma_0 s)\, ds$$
$$= \frac{2k_B T}{\gamma v_0^2}\Big(B + A\exp(\beta t) - (A+B)\exp(-\alpha_2 t)\Big), \tag{24}$$

with $\alpha_2 = 1 + 2\sigma/\tau$, and A, B, and β are as in § 5.1.1. The modified closed-form LED IBVP for the joint PDF p simplifies to

$$\partial_t p + x_2\partial_{x_1} p - x_2\partial_{x_2} p = p + D_2(t)\partial_{x_2x_2} p,$$

where $D_2(t)$ is given by (24). Fig. 2 shows the joint PDF for the semi-local closed-form LED IBVP evolving in time, revealing that the classical (local) LED closure in Fig. 1 induces a faster diffusion rate for the joint PDF.

5.1.3. Nonlocal closure

Employing the PDF method with the *nonlocal closure* to equation (20) results in the closed-form IBVP for the joint PDF p, given by (5), (6), where the cross covariance term (9) is given by

$$\langle \mathbf{v}'\Pi'\rangle \approx -\int_0^t \mathscr{J}(s;\mathbf{X},t)\nabla_{\mathbf{\Phi}}\cdot\Big(\Big\langle \mathbf{v}'(\mathbf{X},t)\mathbf{v}'^T(\mathbf{\Phi}(s;\mathbf{X},t),s)\Big\rangle p(\mathbf{\Phi}(s;\mathbf{X},t),s)]\Big)\, ds$$
$$= -\int_0^t \mathscr{J}(s;\mathbf{X},t)\Big\langle \mathbf{v}'(\mathbf{X},t)\mathbf{v}'^T(\mathbf{\Phi}(s;\mathbf{X},t),s)\Big\rangle \nabla_{\mathbf{\Phi}} p(\mathbf{\Phi}(s;\mathbf{X},t),s)\, ds$$
$$= -\frac{2d}{\tau v_0^2}\int_0^t \exp(t-s)C(\sigma_0 t,\sigma_0 s)\begin{bmatrix} 0 \\ \frac{\partial}{\partial \Phi_2} p(\mathbf{\Phi}(s;\mathbf{X},t),s)\end{bmatrix} ds$$
$$= -\frac{2d}{\tau v_0^2}\int_0^t C(\sigma_0 t,\sigma_0 s)\begin{bmatrix} 0 \\ \partial_{x_2} p(\mathbf{\Phi}(s;\mathbf{X},t),s)\end{bmatrix} ds, \tag{25}$$

where the last equality in (25) results from the substitution of (23). The nonlocal closed-form IBVP for the joint PDF p simplifies to

$$\partial_t p + x_2\partial_{x_1} p - x_2\partial_{x_2} p = p + \nabla_{\mathbf{X}}\cdot\langle \mathbf{v}'\Pi'\rangle(\mathbf{X},t)$$

where

$$\nabla_{\mathbf{X}}\cdot\langle \mathbf{v}'\Pi'\rangle(\mathbf{X},t) \approx -\frac{2d}{\tau v_0^2}\int_0^t C(\sigma_0 t,\sigma_0 s)\partial_{x_2x_2} p(\mathbf{\Phi}(s;\mathbf{X},t),s)\, ds. \tag{26}$$

In order to compare the relative merits of the three considered closures, the marginal PDFs for each closure are computed via quadrature and compared with the Monte Carlo solution of equation (20). Fig. 3 presents two snapshots of the position and velocity marginals for a medium correlation time of $\tau = 10^{-6}$. The local and semi-local closures accurately capture the Monte Carlo solution corresponding to the marginal density of position, i.e. $p(x_1|x_2)$, for the tested correlation times. For the marginal density corresponding to velocity, i.e. $p(x_2|x_1)$, only the semi-local closure retains accuracy in the results of Fig. 3.

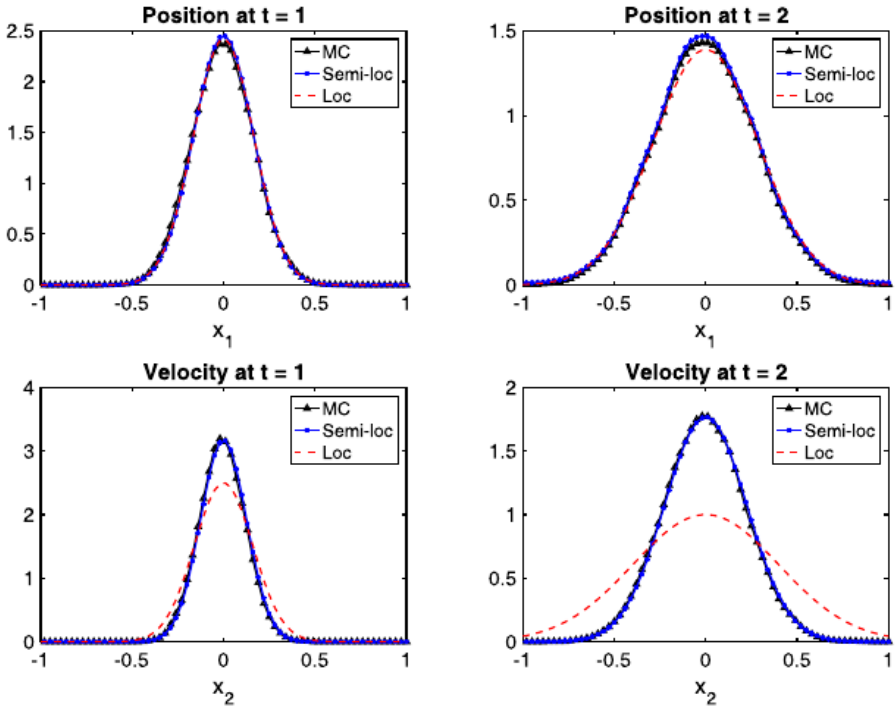

Fig. 3. Comparison of the position (top row) and velocity (bottom row) marginals under local and semi-local closures against Monte-Carlo estimates for the Brownian particle problem with $\tau = 10^{-6}$.

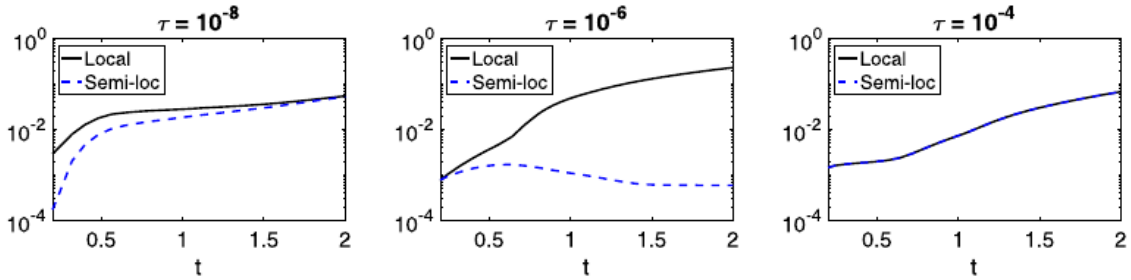

Fig. 4. Evolution of the L^2 error in the velocity marginals under local and semi-local closures for the Brownian particle for correlation times $\tau = 10^{-8}, 10^{-6}$ and 10^{-4}.

More generally, the accuracy of each PDF closure depends on the correlation time τ. We use the L^2-norm of the difference between our approach and the Monte Carlo solution to quantify the error in our approach and refer to that quantity as the L^2 error. For the present Brownian particle example, it was observed that regardless of the correlation time, the nonlocal and semi-local closures are within 10^{-4} from each other in the L^2-norm; therefore, we only report the results from the local and semi-local closures and omit results from the much more computationally expensive nonlocal closure.

As displayed in Fig. 4, in the case of a "large" correlation time of $\tau = 10^{-4}$, results from all three closures are within a 10^{-4} L^2 error. For a small correlation time $\tau = 10^{-8}$, all of the closures agree well with the Monte Carlo solution, with the semi-local and nonlocal closures being slightly more accurate than the local closure. However, for $\tau = 10^{-6}$, the semi-local closure is substantially more accurate than the local closure, see Fig. 4, middle.

The semi-local and nonlocal closures thus lead to results that are significantly more accurate than the local closure. Since the semi-local closure is no less accurate than the nonlocal one and is several orders of magnitude faster than it, we conclude that the semi-local closure is superior to the other two. We re-emphasize that the semi-local approach is also 4 orders of magnitude faster than the Monte Carlo approach.

5.2. Stochastically forced Van der Pol oscillator

We consider a Van der Pol oscillator with stochastic forcing driven by a colored noise

$$\begin{bmatrix} \dot{x}_1 \\ \dot{x}_2 \end{bmatrix} = \begin{bmatrix} x_2 \\ \mu(1 - x_1^2)x_2 - x_1 \end{bmatrix} + \xi_t \begin{bmatrix} 0 \\ \sqrt{\frac{A}{\tau}} \sin(\omega t) \end{bmatrix} \tag{27}$$

where ξ_t is defined by the stochastic differential equation (18) with covariance function $C(t,s)$ given by (19). For our simulations, we take the parameter values as $\mu = 1$, $A = 1$, and $\omega = 5$ and consider three correlation times: $\tau = 0.1$, 1, and 10. The initial condition (6) is taken as an uncorrelated joint Gaussian:

$$p^0 \sim \mathcal{N}\left(\begin{bmatrix}1\\0\end{bmatrix}, \begin{bmatrix}0.01 & 0\\0 & 0.01\end{bmatrix}\right).$$

Unlike in § 5.1, the Jacobian $\mathscr{J}(s;\mathbf{X},t)$ (10) cannot be found exactly since

$$\begin{aligned}\mathscr{J}(s;\mathbf{X},t) &= \exp\left(-\int_s^t \nabla_{\boldsymbol{\chi}} \cdot \langle \mathbf{v}(\boldsymbol{\chi}(\tau),\tau)\rangle \, d\tau\right)\\ &= \exp\left(-\int_s^t \mu(1-\Phi_1^2(\tau;\mathbf{X},t),\tau))\, d\tau\right),\end{aligned}$$

where $\boldsymbol{\Phi}(s;\mathbf{X},t)$ is the solution to the nonlinear terminal problem (7), (8).

To reduce computational cost, we approximate $\boldsymbol{\Phi}(s;\mathbf{X},t)$ in $\mathscr{J}$ by its terminal condition $\mathbf{X}$, resulting in the approximate Jacobian

$$\tilde{\mathscr{J}}(s;\mathbf{X},t) = \exp\left(-\int_s^t \mu(1-x^2)\, d\tau\right) = \exp\left(-\mu(1-x^2)(t-s)\right).$$

5.2.1. Local closure

Applying the PDF method with the *local closure* to equation (27) results in the classical closed-form LED IBVP for the joint PDF p, given by equation (A.14). In this case, the LED drift velocity (A.12) and diffusion tensor (A.13) can be found exactly when approximating $\mathscr{J}$ by $\tilde{\mathscr{J}}$

$$\begin{aligned}\mathscr{V}(\mathbf{X},t) &\equiv \begin{bmatrix}0\\0\end{bmatrix},\\ \mathscr{D}(\mathbf{X},t) &\equiv \int_0^t \tilde{\mathscr{J}}(s;\mathbf{X},t)\left\langle \mathbf{v}'(\mathbf{X},t)\mathbf{v}'^{T}(\boldsymbol{\Phi}(s;\mathbf{X},t),s)\right\rangle ds = D_3(t)\begin{bmatrix}0 & 0\\0 & 1\end{bmatrix},\end{aligned}$$

where

$$D_3(t) = \frac{A\sin(\omega t)}{\tau}\int_0^t \tilde{\mathscr{J}}(s;\mathbf{X},t)C(t,s)\sin(\omega s)\, ds. \tag{28}$$

The integral in equation (28) can be computed analytically (we omit the details). Hence, the classical closed-form LED IBVP for the joint PDF p, given by equation (A.14), simplifies to

$$\partial_t p + x_2\partial_{x_1} p + \left(\mu(1-x_1^2)x_2 - x_1\right)\partial_{x_2} p = -(1-x_1^2)p + D_3(t)\partial_{x_2x_2} p.$$

5.2.2. Semi-local closure

The PDF method, applied to (27) with the *semi-local closure*, results in the closed-form IBVP for the joint PDF p, given by (5), (6), where the cross covariance term is again approximated by (13).

Following [14], we now approximate $\nabla_{\boldsymbol{\Phi}}$ in terms of $\nabla_{\mathbf{X}}$. More precisely, we have

$$\nabla_{\mathbf{X}} = \boldsymbol{\Psi}^T \nabla_{\boldsymbol{\Phi}}, \tag{29}$$

where $\boldsymbol{\Psi}_{ij} = \frac{\partial \boldsymbol{\Phi}_i}{\partial \mathbf{X}_j}(s;\mathbf{X},t)$. We observe through elementary calculus that $\boldsymbol{\Psi}$ satisfies

$$\begin{aligned}\frac{d\boldsymbol{\Psi}}{ds} &= \mathbf{J}\boldsymbol{\Psi},\\ \boldsymbol{\Psi}(t;\mathbf{X},t) &= \mathbb{I},\end{aligned}$$

where $\mathbf{J}$ is the Jacobian of the mean-field velocity, i.e., $\mathbf{J}(\mathbf{Y},s) = \partial\langle\mathbf{v}(\mathbf{Y},s)\rangle/\partial\mathbf{Y}$ and $\mathbb{I}$ is the $N\times N$ identity matrix. Consequently, $\boldsymbol{\Psi}$ can be expressed as

$$\begin{aligned}\boldsymbol{\Psi}(s;\mathbf{X},t) &= OE[\mathbf{J}](s),\\ &= \mathbb{I} + \int_t^s \mathbf{J}(\boldsymbol{\Phi}(s_1;\mathbf{X},t)\,ds_1 + \int_t^s\int_t^{s_1} \mathbf{J}(\boldsymbol{\Phi}(s_1;\mathbf{X},t)\mathbf{J}(\boldsymbol{\Phi}(s_2;\mathbf{X},t)\,ds_1 ds_2 + \dots\end{aligned}$$

where OE is the ordered exponential. By approximating $\mathbf{J}(\boldsymbol{\Phi}(s;\mathbf{X},t)$ by $\mathbf{J}(\mathbf{X},t)$, the ordered exponential simplifies into the matrix exponential and we obtain

$$\boldsymbol{\Psi} \approx \exp((s-t)\mathbf{J}(\mathbf{X},t)),$$

and thus, by (29)

$$\nabla_{\boldsymbol{\Phi}} \approx \exp((t-s)\mathbf{J}(\mathbf{X},t))^T \nabla_{\mathbf{X}}. \tag{30}$$

Using the above substitution and approximating $\mathscr{J}$ by $\tilde{\mathscr{J}}$ in (13) leads to an approximation of the cross covariance term that can be computed analytically

$$\begin{aligned}\langle \mathbf{v}'\Pi' \rangle(\mathbf{X},t) &\approx -\int_0^t \tilde{\mathscr{J}}(s;\mathbf{X},t)\nabla_{\boldsymbol{\Phi}} \cdot \left(\left\langle \mathbf{v}'(\mathbf{X},t)\mathbf{v}'^T(\boldsymbol{\Phi}(s;\mathbf{X},t),s)\right\rangle \tilde{\mathscr{J}}^{-1}(s;\mathbf{X},t)p(\mathbf{X},t)\right) ds\\ &= -\frac{A\sin(\omega t)}{\tau}\int_0^t \tilde{\mathscr{J}}(s;\mathbf{X},t)C(t,s)\sin(\omega s)\begin{bmatrix}0 & 0\\ 0 & 1\end{bmatrix}\exp((t-s)\mathbf{J}(\mathbf{X}))^T \nabla_{\mathbf{X}} \tilde{\mathscr{J}}^{-1}(s;\mathbf{X},t)\; p(\mathbf{X},t)\, ds.\end{aligned} \tag{31}$$

The integrals in (31) can be computed exactly through MAPLE, simplifying the modified closed-form LED IBVP for the joint PDF p to the form:

$$\partial_t p + x_2\partial_{x_1} p + \left(\mu(1-x_1^2)x_2 - x_1\right)\partial_{x_2} p = -(1-x_1^2)p + \partial_{x_2}(D_4\partial_{x_1} p) + \partial_{x_2}(D_5\partial_{x_2} p),$$

where D_4 and D_5 are known functions of x_1, x_2 and t which we omit for brevity. Fig. 5 shows the joint PDF for the semi-local closed-form LED IBVP evolving in time, where the black dots track the ensemble mean. This reveals that the ensemble mean in and of itself does not accurately capture the dynamics of (27).

As with the previous application, we compare the marginal PDFs for each closure obtained via quadrature with the Monte Carlo solution of equation (27). The error plots for the small, medium, and large correlation times are given in Fig. 6. As can be seen there, both the local and semi-local PDF closures agree well with the MC solution for a small correlation time of $\tau = 0.1$ through two pseudo-periods, with the semi-local being slightly more accurate. For a medium correlation time of $\tau = 1$, the local PDF closure captures neither the marginal density for position nor velocity by the end of the first pseudo-period; the semi-local closure is however remarkably accurate for the entire two pseudo-periods. Finally, for the large correlation time of $\tau = 10$, neither the local nor the semi-local closures agree with the MC solution for the entire two pseudo-periods.

We display in Fig. 7 the comparison of the position and velocity marginals against MC for medium ($\tau = 1$) and large ($\tau = 10$) correlation length at roughly the times at which the local closure loses accuracy, i.e., $t = 6$ and $t = 3$ respectively, see Fig. 6.

6. Conclusions

Theoretical analysis and efficient numerical simulation of Langevin equations with colored noise remain an open challenge. The dynamics of Langevin equations can rarely be adequately described by a few low order moments only; this point is clearly illustrated by Fig. 5 where the ensemble mean is often a low probability state. Derivation of Fokker–Planck equations, which describe the dynamics of the probability density function or PDF (rather than its moments), typically requires ad hoc approximations whose validity cannot be ascertained a priori.

The proposed method of distributions demonstrates that the PDF dynamics for Langevin equations with colored noise satisfies a nonlocal (integro-differential) equation that has to be localized in order to derive a Fokker–Planck equation. For white noise, the PDF equations are exact and reduce to their Fokker–Planck counterparts. For colored noise, the derivation of PDF equations requires not only closure approximations but also, for computational convenience, "localization" approximations. We investigate the need and consequences of the latter which takes here the form of the localization of an integro-differential PDF equation. Our analysis leads to the following major conclusions.

- Even though nonlocal (integro-partial-differential) PDF equations are linear, their accurate and reliable numerical resolution is highly challenging in dimensions higher than 2 (the case considered in the paper).
- Localization of such PDF equations yields the "easy-to-solve" (linear, partial-differential) Fokker–Planck equations, but introduces considerable approximation error.

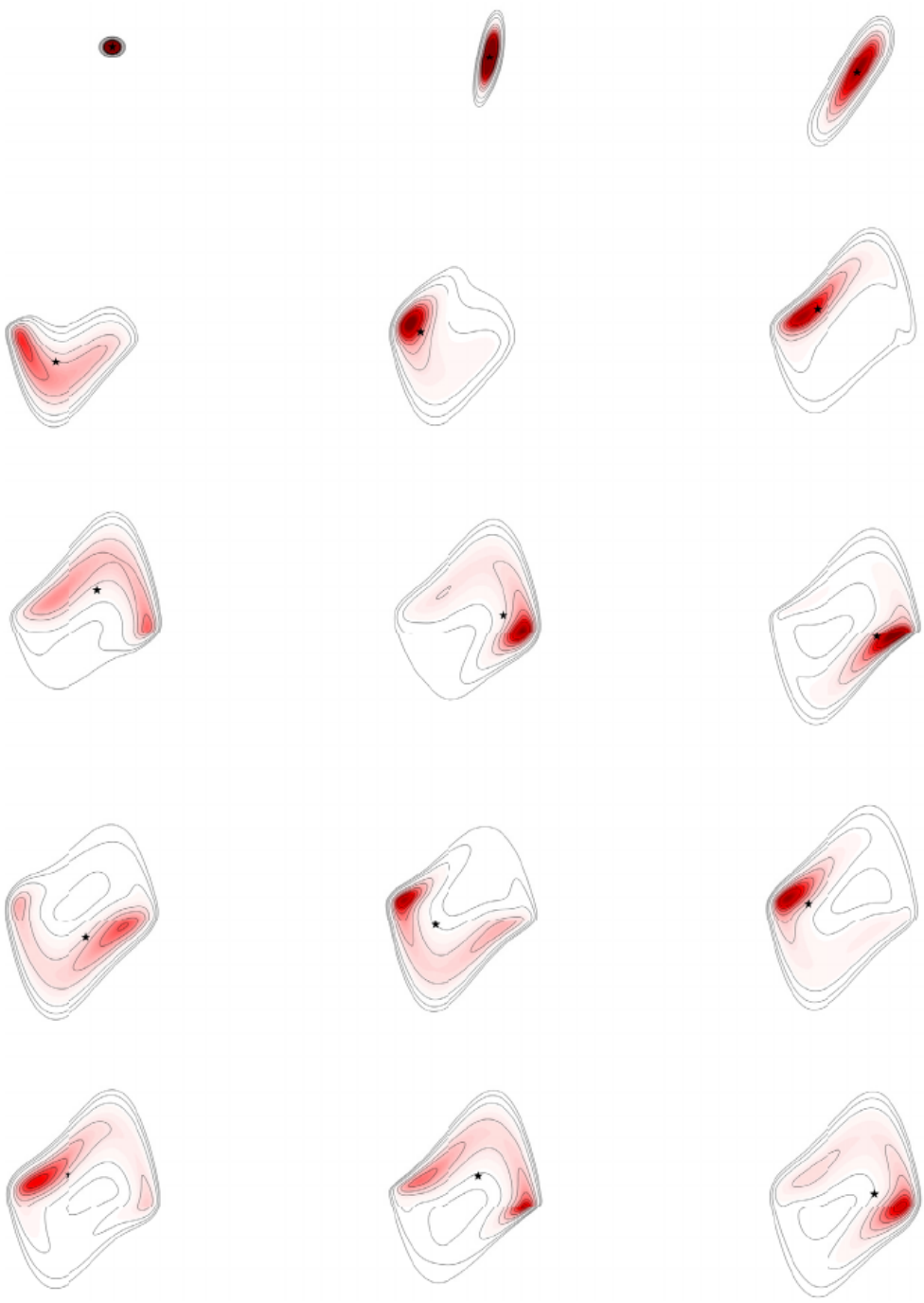

Fig. 5. Evolution of the joint PDF of (27) with $\tau = 0.1$, computed through semi-local closure; the position corresponds to the horizontal axis and the velocity to the vertical one. Time goes from left to right and top to bottom, $t = 0, 0.5, 1, \ldots, 13$. The black dot tracks the ensemble mean.

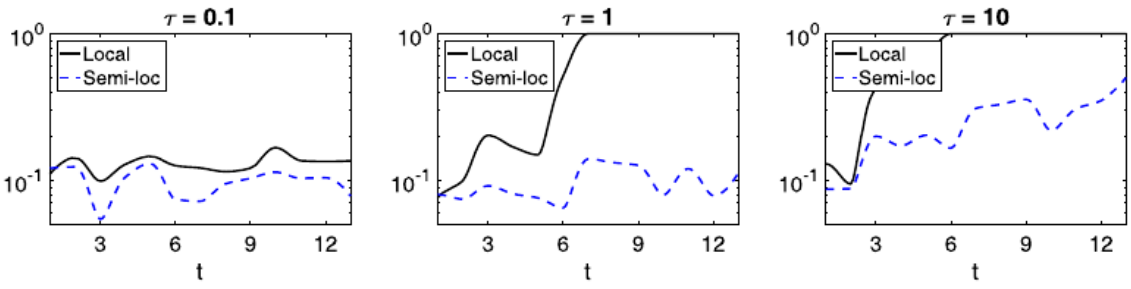

Fig. 6. Evolution of the maximum of the relative L^2 errors in position and in velocity marginals under local and semi-local closures for the stochastically forced Van der Pol oscillator for correlation times $\tau = 10^{-1}, 1$ and 10.

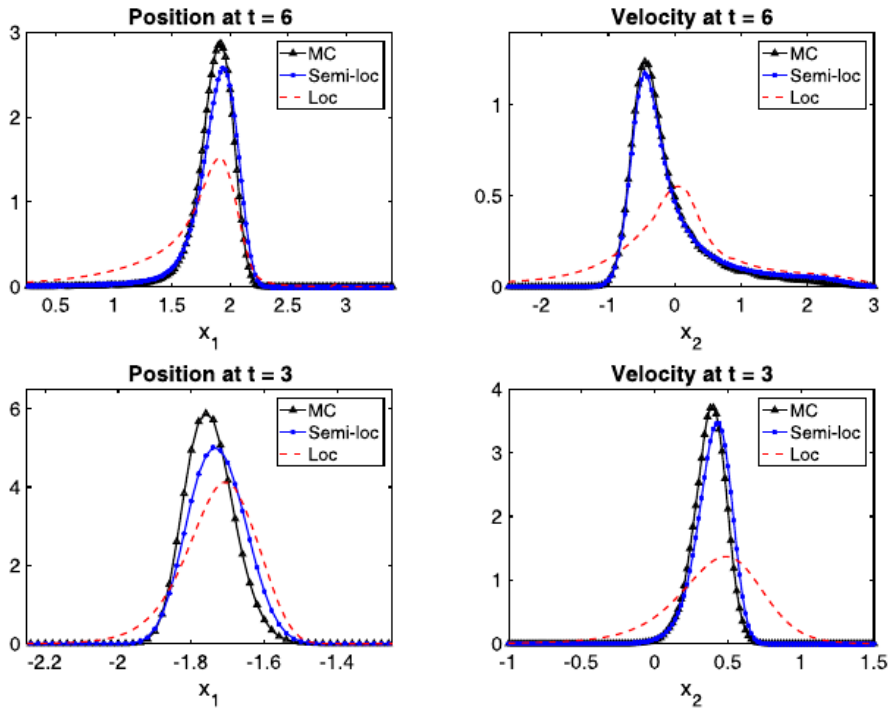

Fig. 7. Comparison of the position and velocity marginals under local and semi-local closures against Monte-Carlo estimates for the stochastically forced Van der Pol oscillator problem; top row: $\tau = 1$, bottom row: $\tau = 10$.

- Partial localization provides an attractive trade-off between accuracy and cost; the sweet spot is likely to be problem dependent.

We use here systems of ODEs driven by colored noise to analyze the localization errors introduced by the LED approximation of otherwise nonlocal PDF equations. However, both PDF equations and their LED-based localizations are equally relevant for first-order (hyperbolic) [2,6,8] and second-order (parabolic) [3] PDEs with random coefficients and/or random driving forces. In a follow up study, we will investigate the localization errors and the use of nonlocal PDF equations in the Partial Differential Equations setting.

Appendix A. Closure derivation

Let L be the linear operator

$$L\Pi = \frac{\partial \Pi}{\partial t} + \nabla_{\mathbf{X}} \cdot (\langle \mathbf{v} \rangle \Pi)$$

together with the initial and boundary conditions

$$\Pi(\mathbf{X}, 0) = \delta(\mathbf{x}^0 - \mathbf{X}) \quad \text{and} \quad \lim_{|\mathbf{X}| \to \infty} \Pi(\mathbf{X}, t) = 0. \tag{A.1}$$

Let $\hat{L}$ be the adjoint of L, i.e.

$$\hat{L}\Psi = -\frac{\partial \Psi}{\partial s} - \langle \mathbf{v} \rangle \cdot \nabla_{\mathbf{Y}} \Psi$$

with vanishing boundary condition at infinity and vanishing terminal condition $\Psi(\mathbf{Y}, t) = 0$. Finally, let $G = G(\mathbf{X}, t; \mathbf{Y}, s)$ be the Green's function of L; G is characterized by

$$\hat{L}G = \delta(\mathbf{X} - \mathbf{Y})\delta(t - s), \tag{A.2}$$

with vanishing boundary condition at infinity and terminal condition $G(\mathbf{X}, t; \mathbf{Y}, t) = 0$. The Green's function G can be obtained through the method of characteristics. Indeed, let's consider the problem

$$\frac{d\boldsymbol{\varphi}}{dr} = \langle \mathbf{v}(\boldsymbol{\varphi}, r) \rangle, \quad r \in (s, t), \tag{A.3}$$

$$\boldsymbol{\varphi}(s) = \mathbf{Y}, \tag{A.4}$$

together with the associated flow $\boldsymbol{\Phi}$, $\boldsymbol{\varphi}(r) = \boldsymbol{\Phi}(r; \mathbf{Y}, s)$. Along the characteristics, the equation for G reduces to

$$\frac{d}{dr} G(\mathbf{X}, t; \boldsymbol{\varphi}, r) = -\delta(t-r)\delta(\mathbf{X} - \boldsymbol{\varphi})$$

with $G(\mathbf{X}, t; \boldsymbol{\Phi}(t; \mathbf{Y}, s), t) = 0$. Integrating in r between s and t, we have

$$G(\mathbf{X}, t; \mathbf{Y}, s) = \mathscr{H}(t-s)\, \delta(\mathbf{X} - \boldsymbol{\Phi}(t; \mathbf{Y}, s)), \tag{A.5}$$

where $\mathscr{H}$ is the Heaviside function. Elementary manipulations lead to the following equation for Π'

$$L\Pi' = -\nabla_{\mathbf{X}} \cdot (\mathbf{v}'\Pi - \langle \mathbf{v}'\Pi' \rangle), \tag{A.6}$$

with homogeneous initial conditions and vanishing boundary conditions. Rewriting (A.6) in terms of $\mathbf{Y}$ and s, multiplying by $G(\mathbf{X}, t; \mathbf{Y}, s)$, and integrating by parts, we obtain

$$\int_0^t \int_{\mathbb{R}^N} GL\Pi' d\mathbf{Y} ds = -\int_{\mathbb{R}^N} G(\mathbf{X}, t; \mathbf{Y}, 0)\Pi'(\mathbf{Y}, 0) d\mathbf{Y} + \int_0^t \int_{\mathbb{R}^N} \Pi' \hat{L} G \, d\mathbf{Y}\, ds,$$

where the additional boundary terms cancel because of the terminal condition on G and the vanishing boundary condition (A.1) at infinity. Taking (A.2) and (A.6) into account leads to

$$\Pi'(\mathbf{X}, t) = \int_{\mathbb{R}^N} G(\mathbf{X}, t; \mathbf{Y}, 0)\Pi'(\mathbf{Y}, 0)\, d\mathbf{Y} + \int_0^t \int_{\mathbb{R}^N} G(\mathbf{X}, t; \mathbf{Y}, s) \nabla_{\mathbf{Y}} \cdot \left(\left\langle \mathbf{v}'(\mathbf{Y}, s)\Pi'(\mathbf{Y}, s) \right\rangle - \mathbf{v}'(\mathbf{Y}, s)\Pi(\mathbf{Y}, s) \right) d\mathbf{Y}\, ds.$$

The initial time term on the right vanishes if the initial condition on $\mathbf{x}^0$ is deterministic. We obtain an exact (unclosed) equation for the stochastic flux $\langle \mathbf{v}'\Pi' \rangle$ by multiplying the previous relation by $\mathbf{v}'(\mathbf{X}, t)$ and taking the ensemble mean

$$\langle \mathbf{v}'\Pi' \rangle(\mathbf{X}, t) = \int_{\mathbb{R}^N} G(\mathbf{X}, t; \mathbf{Y}, 0) \langle \mathbf{v}'(\mathbf{X}, t)\Pi'(\mathbf{Y}, 0) \rangle\, d\mathbf{Y} - \int_0^t \int_{\mathbb{R}^N} G(\mathbf{X}, t; \mathbf{Y}, s) \nabla_{\mathbf{Y}} \cdot \left\langle \mathbf{v}'(\mathbf{X}, t) \mathbf{v}'^{T}(\mathbf{Y}, s)\Pi(\mathbf{Y}, s) \right\rangle d\mathbf{Y}\, ds.$$

The LED closure corresponds here to assuming $\Pi' \approx 0$ on the right hand side of the above equation, resulting in a computable relationship

$$\langle \mathbf{v}'\Pi' \rangle(\mathbf{X}, t) \approx -\int_0^t \int_{\mathbb{R}^N} G(\mathbf{X}, t; \mathbf{Y}, s) \nabla_{\mathbf{Y}} \cdot \left(\left\langle \mathbf{v}'(\mathbf{X}, t) \mathbf{v}'^{T}(\mathbf{Y}, s) \right\rangle p(\mathbf{Y}, s) \right) d\mathbf{Y}\, ds. \tag{A.7}$$

Setting

$$q(\mathbf{X}, \mathbf{Y}, t, s) = \nabla_{\mathbf{Y}} \cdot \left(\left\langle \mathbf{v}'(\mathbf{X}, t) \mathbf{v}'^{T}(\mathbf{Y}, s) \right\rangle p(\mathbf{Y}, s) \right),$$

expression (A.7) can be simplified by taking into account the form (A.5) of G

$$\begin{aligned} \langle \mathbf{v}'\Pi' \rangle(\mathbf{X}, t) &\approx -\int_0^t \int_{\mathbb{R}^N} \delta(\mathbf{X} - \boldsymbol{\Phi}(t; \mathbf{Y}, s))\, q(\mathbf{X}, \mathbf{Y}, t, s)\, d\mathbf{Y}\, ds, \\ &\approx -\int_0^t \int_{\mathbb{R}^N} \delta(\mathbf{X} - \boldsymbol{\varphi})\, q(\mathbf{X}, \boldsymbol{\Phi}(s; \boldsymbol{\varphi}, t), t, s) \left| \frac{d\boldsymbol{\Phi}(s; \boldsymbol{\varphi}, t)}{d\boldsymbol{\varphi}} \right| d\mathbf{Y}\, ds. \end{aligned}$$

The expression of the Jacobian from the previous relation can be made explicit by invoking the Liouville–Ostrogradski Lemma which we recall and prove below (not having been able to find an appropriate reference to it in the literature).

Lemma 1 *(Liouville–Ostrogradski). Consider the initial value problem*

$$\frac{d\boldsymbol{\chi}}{ds} = \mathbf{f}(\boldsymbol{\chi}, s), \tag{A.8}$$

$$\boldsymbol{\chi}(t) = \boldsymbol{\xi}, \tag{A.9}$$

where $\mathbf{f}:\mathbb{R}^N\times\mathbb{R}\to\mathbb{R}^N$ *is a given deterministic function and* $\boldsymbol{\xi}$ *a possibly random initial condition. Both* $\mathbf{f}$ *and* $\boldsymbol{\xi}$ *are assumed to be such that, for any realization of* $\boldsymbol{\xi}$*, the above system admits a unique solution for the range of time under consideration. Then, if* $\boldsymbol{\Phi}$ *is the corresponding flow, i.e.,* $\boldsymbol{\chi}(s)=\boldsymbol{\Phi}(s;\boldsymbol{\xi},t)$*, we have*

$$\left|\frac{\partial\boldsymbol{\Phi}(s;\boldsymbol{\xi},t)}{\partial\boldsymbol{\xi}}\right|=\exp\left(-\int_s^t\nabla_{\boldsymbol{\chi}}\cdot\mathbf{f}(\boldsymbol{\chi}(\tau),\tau)\,d\tau\right).$$

Proof. Proceeding similarly to § 2, it is straightforward to check that p, the PDF of $\boldsymbol{\chi}$, satisfies

$$\frac{\partial p}{\partial t}+\nabla_{\boldsymbol{\chi}}\cdot(\mathbf{f}p)=0.$$

We define $\mathcal{P}(s)=p(\boldsymbol{\chi}(s),s)$ as the restriction of p on characteristic curves. By construction, $\mathcal{P}$ satisfies

$$\frac{d\mathcal{P}}{ds}=-\mathcal{P}\,\nabla_{\boldsymbol{\chi}}\cdot\mathbf{f},$$

and thus by integration

$$\mathcal{P}(s)=\mathcal{P}(t)\exp\left(-\int_t^s\nabla_{\boldsymbol{\chi}}\cdot\mathbf{f}(\boldsymbol{\chi}(\tau),\tau)d\tau\right).$$

The flow $\boldsymbol{\Phi}$ can be regarded as a one-to-one change of variables and thus

$$\mathcal{P}(s)=\left|\frac{d}{d\boldsymbol{\chi}}\boldsymbol{\Phi}^{-1}\right|\mathcal{P}(t).$$

Plugging into the previous relation and taking the inverse completes the proof. □

We apply the Liouville–Ostrogradski lemma with $\boldsymbol{\chi}$ and $\boldsymbol{\Phi}$ being respectively the solution and the flow corresponding to (A.8) and (A.9) with $\mathbf{f}(\chi,s)=\langle\mathbf{v}(\boldsymbol{\chi},s)\rangle$ and $\boldsymbol{\varphi}=\boldsymbol{\xi}=\mathbf{X}$; this yields

$$\langle\mathbf{v}'\Pi'\rangle(\mathbf{X},t)\approx-\int_0^t\mathscr{J}(s;\mathbf{X},t)\nabla_{\boldsymbol{\Phi}}\cdot\left(\left\langle\mathbf{v}'(\mathbf{X},t)\mathbf{v}'^{T}(\boldsymbol{\Phi}(s;\mathbf{X},t),s)\right\rangle p(\boldsymbol{\Phi}(s;\mathbf{X},t),s)\right)ds,\tag{A.10}$$

where

$$\mathscr{J}(s;\mathbf{X},t)=\exp\left(-\int_s^t\nabla_{\boldsymbol{\chi}}\cdot\langle\mathbf{v}(\boldsymbol{\chi}(\tau),\tau)\rangle\,d\tau\right).$$

Substituting approximation (A.10) into (5) gives a time-convoluted integro-differential equation for p resulting from colored noise. The integro-differential equation can be solved numerically but may pose significant numerical challenges as the resulting problem is local neither in time nor in space.

The localization inherent in the classical LED theory [7]ignores the variation of p over the correlation time interval. In other words, it assumes that p and its spatial derivatives are approximately uniform over the interval $(t-\tau,t)$. This gives rise to approximations $p(\boldsymbol{\Phi}(s;\mathbf{X},t),s)\approx p(\mathbf{X},t)$ and $\nabla_{\boldsymbol{\Phi}}p(\boldsymbol{\Phi}(s;\mathbf{X},t),s)\approx\nabla_{\mathbf{X}}p(\mathbf{X},t)$, so that

$$\langle\mathbf{v}'\Pi'\rangle(\mathbf{X},t)\approx\mathscr{V}(\mathbf{X},t)p(\mathbf{X},t)-\mathscr{D}(\mathbf{X},t)\nabla_{\mathbf{X}}p(\mathbf{X},t),\tag{A.11}$$

where $\mathscr{V}$ and $\mathscr{D}$ are the LED drift velocity and diffusion tensor

$$\mathscr{V}(\mathbf{X},t)\equiv-\int_0^t\mathscr{J}(s;\mathbf{X},t)\left\langle\mathbf{v}'(\mathbf{X},t)\nabla_{\boldsymbol{\Phi}}\cdot\mathbf{v}'^{T}(\boldsymbol{\Phi}(s;\mathbf{X},t),s)\right\rangle ds,\tag{A.12}$$

$$\mathscr{D}(\mathbf{X},t)\equiv\int_0^t\mathscr{J}(s;\mathbf{X},t)\left\langle\mathbf{v}'(\mathbf{X},t)\mathbf{v}'^{T}(\boldsymbol{\Phi}(s;\mathbf{X},t),s)\right\rangle ds.\tag{A.13}$$

Substituting (A.11), (A.12), (A.13) into (5) results in the following classical closed-form LED IBVP for the joint probability density function p:

$$\frac{\partial p}{\partial t} + \nabla_{\mathbf{x}} \cdot \Big((\langle \mathbf{v} \rangle + \mathscr{V}) p \Big) = \nabla_{\mathbf{x}} \cdot (\mathscr{D} \nabla_{\mathbf{x}} p). \tag{A.14}$$

The shortcomings of the above LED closure–mostly importantly, its limited validity to short correlation timescale–are well known and documented [14].

References

[1] T.S. Lundgren, Distribution functions in the statistical theory of turbulence, Phys. Fluids 10 (5) (1967) 969–975.
[2] D.M. Tartakovsky, P.A. Gremaud, Method of distributions for uncertainty quantification, in: R. Ghanem (Ed.), Handbook of Uncertainty Quantification, Springer, 2015, pp. 1–22.
[3] F. Boso, D.M. Tartakovsky, The method of distributions for dispersive transport in porous media with uncertain hydraulic properties, Water Resour. Res. 52 (6) (2016) 4700–4712, https://doi.org/10.1002/2016WR018745.
[4] P. Wang, A.M. Tartakovsky, D.M. Tartakovsky, Probability density function method for Langevin equations with colored noise, Phys. Rev. Lett. 110 (14) (2013) 140602, https://doi.org/10.1103/PhysRevLett.110.140602.
[5] D. Venturi, T.P. Sapsis, H. Cho, G.E. Karniadakis, A computable evolution equation for the joint response-excitation probability density function of stochastic dynamical systems, Proc. R. Soc. A 468 (2139) (2012) 759–783.
[6] D. Venturi, D.M. Tartakovsky, A.M. Tartakovsky, G.E. Karniadakis, Exact PDF equations and closure approximations for advective–reactive transport, J. Comput. Phys. 243 (2013) 323–343, https://doi.org/10.1016/j.jcp.2013.03.001.
[7] R.H. Kraichnan, Eddy viscosity and diffusivity: exact formulas and approximations, Complex Syst. 1 (1987) 805–820.
[8] D.M. Tartakovsky, S. Broyda, PDF equations for advective–reactive transport in heterogeneous porous media with uncertain properties, J. Contam. Hydrol. 120–121 (2011) 129–140.
[9] S.P. Neuman, D.M. Tartakovsky, Perspective on theories of anomalous transport in heterogeneous media, Adv. Water Resour. 32 (5) (2009) 670–680, https://doi.org/10.1016/j.advwatres.2008.08.005.
[10] D.M. Tartakovsky, S.P. Neuman, Transient flow in bounded randomly heterogeneous domains, 2: localization of conditional mean equations and temporal nonlocality effects, Water Resour. Res. 34 (1) (1998) 13–20.
[11] S. Hottovy, G. Volpe, J. Wehr, Thermophoresis of Brownian particles driven by coloured noise, Europhys. Lett. 99 (2012) 60002.
[12] J. Strand, Random ordinary differential equations, J. Differ. Equ. 7 (1970) 538–553.
[13] T. Neckel, F. Rupp, Random Differential Equations in Scientific Computing, De Gruyter, 2013.
[14] D. Barajas-Solano, A. Tartakovsky, Probabilistic density function method for nonlinear dynamical systems driven by colored noise, Phys. Rev. E 93 (2016) 052121.
[15] H. Cho, D. Venturi, G. Karniadakis, Adaptive discontinuous Galerkin method for response-excitation PDF equations, SIAM J. Sci. Comput. 35 (2013) B890–B911.
[16] Clawpack Development Team, Clawpack software, version 5.3.1, http://www.clawpack.org, 2015.
[17] T. Li, M. Raizen, Brownian motion at short time scales, Ann. Phys. (2013) 1–15.